

# Design of Robust PI Controller for Vehicle Suspension System

Celaleddin Yeroglu\* and Nusret Tan\*

**Abstract** – This paper deals with the design of a robust PI controller for a vehicle suspension system. A method, which is related to computation of all stabilizing PI controllers, is applied to the vehicle suspension system in order to obtain optimum control between passenger comfort and driving performance. The PI controller parameters are calculated by plotting the stability boundary locus in the  $(k_p, k_i)$ -plane and illustrative results are presented. In reality, like all physical systems, the vehicle suspension system parameters contain uncertainty. Thus, the proposed method is also used to compute all the parameters of a PI controller that stabilize a vehicle suspension system with uncertain parameters.

**Keywords:** Gain and phase margins, PI control, Robustness analysis, Stabilization, Uncertain systems, Vehicle suspension system

## 1. Introduction

Nowadays, progress in the automobile industry is very impressive. Automobile manufacturers aim to increase passenger comfort besides increasing driving safety and performance. Therefore, vehicle suspension is essential in order to guarantee a high safety factor and ride comfortability. Moreover, suspension modeling is very important for a realistic suspension control design [1-3]. Passive suspension systems, which are designed by placing a spring and a diminishing element between the wheel and the body of the vehicle, allow forward compensation between the driving comfort and deviation of the suspension stroke. Because of the structural features of the vehicles, the suspension stroke is limited between the specified values. Thus, if suspension deviation reaches these limit values, it causes reduced driving comfort. Active suspension systems are designed by placing a hydraulic system, which is controlled by feedback controller, between the wheel and the body of the vehicle. The suspension system controllers, which are designed by using linear control methods, allow forward compensation between the driving comfort and performance criteria of deviation of the suspension [4-7]. Several types of controllers like LQR control,  $H_\infty$  control, P, PI, and PID are used for the design of vehicle suspension systems [1-9]. On the other hand, in recent years, there have been some new developments in the design of control systems. Especially, there is a growing interest of calculating all stabilizing P, PI, and PID controllers [10-19]. These control

methods can be useful for the design of suspension systems.

In this paper, the stability boundary locus method [15] is applied to a vehicle suspension system. All stabilizing PI controllers are obtained for the system using this approach. Equations for  $k_p$  and  $k_i$  parameters are derived and the stability boundary of the system is obtained using these equations. Then, the stability regions for required gain and phase margins are identified. It is known that, like all physical systems, vehicle suspension systems also include uncertainties. Thus, robustness analysis of the system becomes very important and must be considered. In this paper, in order to achieve a more realistic design, the robust stability region of the system is identified by using the Kharitonov theorem [20-21] and the stability boundary locus approach. The method presented in this paper enables one to design a robust PI controller for a vehicle suspension system by using the derived formulas and investigated stability regions.

The paper is organized as follows: The proposed method for controller stabilization and the design of PI controllers that achieve user specified gain and phase margins is given in Section 2. A suspension system for the quarter car model and PI controller design for the model is provided in Section 3. In Section 4, robustness analysis of the system is studied. Conclusions are offered in Section 5.

## 2. Stabilization for Specified Gain and Phase Margins Using a PI Controller

Consider the single-input single-output (SISO) control system of Fig. 1 where

\* Dept. of Electrical and Electronic Engineering, Inonu University, Turkey. (cyeroglu@inonu.edu.tr), (ntan@inonu.edu.tr)  
Received 19 September, 2007 ; Accepted 23 January, 2008

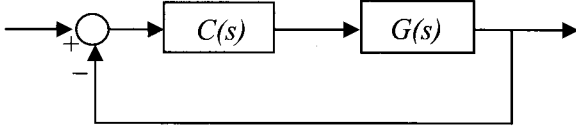


Fig. 1. A SISO control system

$$G(s) = \frac{N(s)}{D(s)} \quad (1)$$

is the plant to be controlled and  $C(s)$  is a PI controller of the form

$$C(s) = k_p + \frac{k_i}{s} = \frac{k_p s + k_i}{s} \quad (2)$$

The problem is to compute the parameters of the PI controller of Eq. (2) which stabilize the system of Fig. 1.

Decomposing the numerator and the denominator polynomials of Eq. (1) into their even and odd parts, and substituting  $s = j\omega$ , gives

$$G(j\omega) = \frac{N_e(-\omega^2) + j\omega N_o(-\omega^2)}{D_e(-\omega^2) + j\omega D_o(-\omega^2)} \quad (3)$$

The closed loop characteristic polynomial of the system can be written as

$$\begin{aligned} \Delta(j\omega) &= \\ & [k_i N_e(-\omega^2) - k_p \omega^2 N_o(-\omega^2 - \omega^2 D_o(-\omega^2))] \quad (4) \\ & + j[k_p \omega N_e(-\omega^2) + k_i \omega N_o(-\omega^2) + \omega D_e(-\omega^2)] \\ & = R_\Delta + jI_\Delta = 0 \end{aligned}$$

Then, equating the real and imaginary parts of  $\Delta(j\omega)$  to zero, one obtains

$$k_p(-\omega^2 N_o(-\omega^2)) + k_i(N_e(-\omega^2)) = \omega^2 D_o(-\omega^2) \quad (5)$$

And

$$k_p(\omega N_e(-\omega^2)) + k_i(\omega N_o(-\omega^2)) = -\omega D_e(-\omega^2) \quad (6)$$

Solving these equations, it can be found that

$$k_p = \frac{\omega^2 N_o D_e + N_e D_e}{-(N_e^2 + \omega^2 N_o^2)} \quad (7)$$

and

$$k_i = \frac{\omega^2(N_o D_e - N_e D_o)}{-(N_e^2 + \omega^2 N_o^2)} \quad (8)$$

Thus, the stability boundary locus,  $l(k_p, k_i, \omega)$ , in the  $(k_p, k_i)$ -plane can be obtained using Eqs. (7) and (8). The stability boundary locus,  $l(k_p, k_i, \omega)$ , and the line  $k_i = 0$  (since a real root of  $\Delta(s)$  of Eq. (4) can cross the imaginary axis at  $s = 0$ ), thus, for  $\omega = 0$ ,  $I_\Delta = 0$  and from  $R_\Delta = 0$  it can be found that  $(k_i = 0)$  divides the parameter plane ( $(k_p, k_i)$ -plane) into stable and unstable regions. Choosing a test point within each region, the stable region that contains the values of stabilizing  $k_p$  and  $k_i$  parameters can be determined. Phase and gain margins are two important frequency domain performance measures that are widely used in classical control theory for controller design. Consider Fig. 1 with a gain-phase margin tester,  $G_c(s) = A e^{-j\phi}$ , which is connected in the feed forward path. Then,

$$k_p = \frac{(\omega^2 N_o D_e + N_e D_e) \cos(h) + \omega(N_o D_e - N_e D_o) \sin(h)}{-A(N_e^2 + \omega^2 N_o^2)} \quad (9)$$

And

$$k_i = \frac{\omega^2(N_o D_e - N_e D_o) \cos(h) - \omega(N_e D_e + \omega^2 N_o D_o) \sin(h)}{-A(N_e^2 + \omega^2 N_o^2)} \quad (10)$$

where  $h = \omega\tau + \phi$ . To obtain the stability boundary locus for a given value of gain margin  $A$ , one needs to set  $\phi = 0$  in Eqs. (9) and (10). On the other hand, setting  $A = 1$  in Eqs. (9) and (10), one can obtain the stability boundary locus for a given phase margin  $\phi$ . The details of the method can be found in [15].

### 3. Vehicle Suspension System

#### 3.1 Derivation of the Transfer Function

The words, sentences, and results given in this subsection are completely taken from the textbook by Franklin et al. [22, pp. 26-29]. Consider a vehicle with a four-wheel suspension system. A system comprised of one wheel having suspension is usually referred to as a quarter-car model. Let's assume a car model has a mass of 1000 kg including the four wheels, which have a mass of 20 kg each. By placing a known weight directly over a wheel and measuring the car's deflection, it can be found that  $k_s = 130.000 N/m$ ,  $k_w \cong 1.000.000 N/m$ . and  $b = 9800 N \cdot sec/m$ . [22] A vehicle suspension system can be approximated by the simplified system as shown in

Fig. 2. The coordinates of the two masses,  $x$  and  $y$ , with the reference direction as shown, are the displacements of the masses from their equilibrium conditions. The equilibrium positions are offset from the springs' unstretched positions because of the force of gravity. The shock absorber is represented in the schematic diagram by a dashpot symbol with friction constant  $b$ . The magnitude of the force from the shock absorber is assumed to be proportional to the rate of change of the relative displacement of the two masses, that is, to  $b(\dot{y} - \dot{x})$ . The force of gravity could be included in the free body diagram; however, its effect is to produce a constant offset of  $x$  and  $y$ . By defining  $x$  and  $y$  to be the distance from the equilibrium position, the need to include the gravity forces is eliminated.

Force from the car suspension acts on both masses in proportion to their relative displacement with spring constant  $k_s$ . Fig. 2 shows the free body diagram of each mass. Note that the force from the spring on the two masses is equal in magnitude but acts in opposite directions, which is also the case for the damper. A positive displacement  $y$  of mass  $m_2$  will result in a force from the spring on  $m_2$  in the direction shown. However, a positive displacement  $x$  of mass  $m_1$  will result in a force from the spring  $k_s$  on  $m_1$  in the opposite direction to that drawn in Fig. 3 as indicated by the minus  $x$ -term for the spring force.

The lower spring  $k_w$  represents the tire compressibility, for which there is insufficient damping (velocity-dependent force) to warrant including a dashpot in the model. The force from this spring is proportional to the distance the tire is compressed and the nominal equilibrium force would be that required to support  $m_1$  and  $m_2$  against gravity. By defining  $x$  to be the distances from equilibrium, a force will result if either the road surface has a bump (changes from its equilibrium value of zero) or the wheel bounces ( $x$  changes). The motion of the simplified car over a bumpy road will result in a value of  $r(t)$  that is not constant. As noted above, there is a constant force of gravity acting on each mass; however such force has been omitted, as have the equal and opposite forces from the springs. Gravitational forces can always be omitted from vertical-spring mass systems, if the position coordinates are defined from the equilibrium position that results when gravity is acting and if the spring forces used in the analysis are actually the perturbation in spring forces from those forces acting at equilibrium.

Applying Newton's Law to each mass and noting that some forces on each mass are in the negative (down) direction yields the system of equations

$$b(\dot{y} - \dot{x}) + k_s(y - x) - k_w(x - r) = m_1\ddot{x}, \quad (11)$$

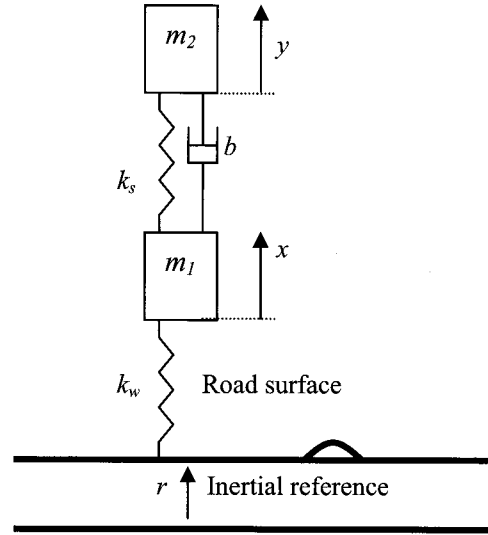


Fig. 2. The quarter car model

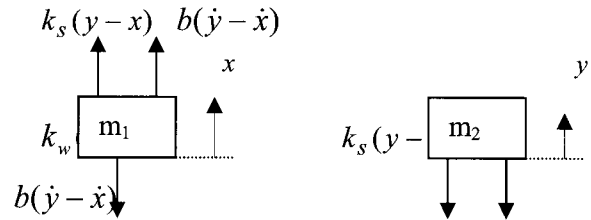


Fig. 3. Free-body diagram for suspension system.

$$-k_s(y - x) - b(\dot{y} - \dot{x}) = m_2\ddot{y} \quad (12)$$

Some rearranging results in

$$\ddot{x} + \frac{b}{m_1}(\dot{x} - \dot{y}) + \frac{k_s}{m_1}(x - y) + \frac{k_w}{m_1}x = \frac{k_w}{m_1}r, \quad (13)$$

$$\ddot{y} + \frac{b}{m_2}(\dot{y} - \dot{x}) + \frac{k_s}{m_2}(y - x) = 0 \quad (14)$$

Taking Laplace transforms of Eqs. (13) and (14), and assuming that initial conditions are equal to zero yields,

$$s^2X(s) + s\frac{b}{m_1}(X(s) - Y(s)) + \frac{k_s}{m_1}(X(s) - Y(s)) + \frac{k_w}{m_1}X(s) = \frac{k_w}{m_1}R(s) \quad (15)$$

$$s^2Y(s) + s\frac{b}{m_2}(Y(s) - X(s)) + \frac{k_s}{m_2}(Y(s) - X(s)) = 0 \quad (16)$$

and after some algebra and rearranging yields the transfer function,

$$\frac{Y(s)}{R(s)} = \frac{\frac{k_w b}{m_1 m_2} (s + \frac{k_s}{b})}{s^4 + (\frac{b}{m_1} + \frac{b}{m_2})s^3 + (\frac{k_s}{m_1} + \frac{k_s}{m_2} + \frac{k_w}{m_1})s^2 + (\frac{k_w b}{m_1 m_2})s + \frac{k_w k_s}{m_1 m_2}} \quad (17)$$

To determine numerical values, we subtract the mass of the four wheels from the total car mass of 1000 kg. and divide by 4 to find that  $m_2 = 250\text{kg}$ . The wheel mass was measured directly to be  $m_1 = 20\text{kg}$ . Therefore, the transfer function with the numerical values is

$$\frac{Y(s)}{R(s)} = G(s) = \frac{1.96 \times 10^6 s + 2.6 \times 10^7}{s^4 + (529.2)s^3 + 57020s^2 + 1.96 \times 10^6 s + 2.6 \times 10^7} \quad (18)$$

### 3.2 Design of Robust PI Controller for Vehicle Suspension System

In order to apply the stability boundary locus technique to the vehicle suspension system given in Eq. (18) one can find  $k_p$  and  $k_i$  parameters that are given in Eqs. (7) and (8) as below.

$$k_p = \frac{1.011232 \times 10^9 \omega^4 - 2.35908 \times 10^{12} \omega^2 - 6.76 \times 10^{14}}{3.8416 \times 10^{12} \omega^2 + 6.76 \times 10^{14}} \quad (19)$$

And

$$k_i = \frac{-1.96 \times 10^6 \omega^6 + 9.8 \times 10^{10} \omega^4}{3.8416 \times 10^{12} \omega^2 + 6.76 \times 10^{14}} \quad (20)$$

The aim is to compute all the stabilizing values of  $k_p$  and  $k_i$  which cause the characteristic polynomial of Eq. (4) to be Hurwitz stable. For range of frequency, the stability boundary locus can be easily computed. For example, for  $\omega \in [0, 240]$ ,  $l(k_p, k_i, \omega)$  is shown in Fig. 4.

From this figure it can be seen that there are a few regions, namely R1, R2, and R3, in which one needs to choose a test point in order to find the stability region. For example, choosing a test point within region R3 such as  $k_p = 12$  and  $k_i = 300$ , it can be calculated that the characteristic polynomial has two right half plane complex roots that are  $8.87 \pm 216.44j$ , therefore, the system is unstable for these values of parameters. Thus, the region R3 is not a stable region. It is found that the only stabilizing region is the region denoted by R1. For example, for  $k_p = 5$  and  $k_i = 100$ , within region R1, the characteristic polynomial can be calculated as

$$\Delta(s) = s^5 + 5.292 \times 10^2 s^4 + 5.702 \times 10^4 s^3 + 1.176 \times 10^7 s^2 + 3.52 \times 10^8 s + 2.6 \times 10^9 \quad (21)$$

which is a stable polynomial. Fig. 5 demonstrates more clearly R1 for all stabilizing values of  $k_p$  and  $k_i$ .

The proposed method is very fast and effective for finding the stability region for the parameters of suspension system. An efficient approach to reduce the range of frequency, which needs to be grided, can be obtained by using the Nyquist plot based approach of [16]. In this case, it is only necessary to find real values of  $\omega$  that satisfy  $\text{Im}[G(s)] = 0$  where  $s = j\omega$ . Thus, the frequency axis can be divided into a finite number of intervals and then by testing each interval the stability region can be computed. For the suspension system it can be calculated that the only real frequency value that satisfies  $\text{Im}[G(j\omega)] = 0$  is  $223.6 \text{ rad/sec}$ . Thus, the frequency axis can be divided into two intervals such as  $\omega \in (0, 223.6)$  and  $\omega \in (223.6, \infty)$ . For 2240 points within  $\omega \in [0, 240]$ ,  $l(k_p, k_i, \omega)$  is revealed in Fig. 4 where it can be seen that there are stabilizing values of  $k_p$  and  $k_i$  when  $\omega \in (0, 223.6)$ .

To find all stabilizing PI controller parameters for the suspension model, which satisfies the conditions that the phase margin of the system is greater than  $45^\circ$  and the gain margin is greater than 3 (9.54 db), first let us compute the stability boundary locus. Using Eqs. (9) and (10),

$$k_p = \frac{N_A \cos \phi + N_B \sin \phi}{-A(3.8416 \times 10^{12} \omega^2 + 6.76 \times 10^{14})} \quad (22)$$

$$k_i = \frac{\omega N_B \cos \phi - \omega N_A \sin \phi}{-A(3.8416 \times 10^{12} \omega^2 + 6.76 \times 10^{14})} \quad (23)$$

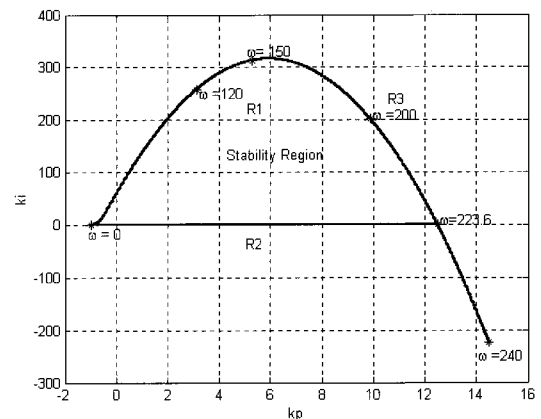


Fig. 4. Stability boundary locus of suspension system for  $\omega \in [0, 240]$

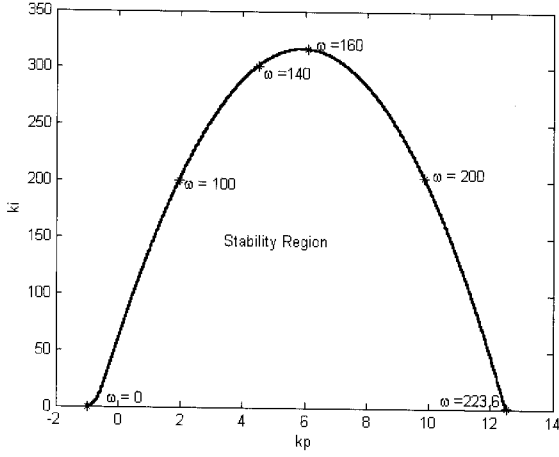


Fig. 5. All stabilizing PI controllers

where,

$$N_A = -1.011232 \times 10^9 \omega^4 + 2.35908 \times 10^9 \omega^2 + 6.76 \times 10^{14}$$

$$N_B = 1.96 \times 10^6 \omega^5 - 9.8 \times 10^{10} \omega^3$$

For  $A=1$  and  $\phi=0$ , since  $\text{Im}[G(j\omega)] = 0$  for  $\omega = 223.6$  rad/sec, it is only necessary to grid  $\omega$  within  $\omega \in (0, 223.6)$ . The stabilizing region is shown in Fig. 5. To find all stabilizing PI controllers for which the phase margin of the system is greater than  $45^\circ$ , it is required to set  $A=1$  and  $\phi=45^\circ$  in Eq. (22) and (23). Using Eqs. (9) and (10), for these values of  $A$  and  $\phi$  gives

$$k_p = \frac{1.96 \times 10^6 \omega^5 - 1.011232 \times 10^9 \omega^4 - 9.8 \times 10^{10} \omega^3 + 2.35908 \times 10^9 \omega^2 + 6.76 \times 10^{14}}{-5.416656 \times 10^{12} \omega^2 - 9.5316 \times 10^{14}} \quad (24)$$

and

$$k_i = \frac{1.96 \times 10^6 \omega^6 + 1.011232 \times 10^9 \omega^5 - 9.8 \times 10^{10} \omega^4 - 2.35908 \times 10^9 \omega^3 - 6.76 \times 10^{14} \omega}{-5.416656 \times 10^{12} \omega^2 - 9.5316 \times 10^{14}} \quad (25)$$

The range of  $\omega$  needed for stabilization for this case can be found from  $G(j\omega) = 45^\circ$ . It can be calculated that  $\arg[G(j\omega)] = -135^\circ$  for  $\omega = 101$  rad/sec. The stability boundary locus for  $\phi = 45^\circ$  with  $\omega$  varying within  $\omega \in (0, 101)$  is shown in Fig. 6. Similarly, setting  $\phi = 0$  and  $A = 3$  in Eqs. (22) and (23), it is found that

$$k_p = \frac{-1.011232 \times 10^9 \omega^4 + 2.35908 \times 10^9 \omega^2 + 6.76 \times 10^{14}}{-5.416656 \times 10^{12} \omega^2 - 9.5316 \times 10^{14}} \quad (26)$$

and

$$k_i = \frac{1.96 \times 10^6 \omega^6 - 9.8 \times 10^{10} \omega^4}{-5.416656 \times 10^{12} \omega^2 - 9.5316 \times 10^{14}} \quad (27)$$

The stability boundary locus for  $A=3$  can be obtained for  $\omega \in (0, 223.6)$  as presented in Fig. 6. The region obtained from the intersections of these regions includes the stabilizing values of  $k_p$  and  $k_i$  which make the phase margin of the system greater than  $45^\circ$  and the gain margin greater than 3. For example, choosing a point in the region such as  $k_p = 1.5$  and  $k_i = 10$ , it can be computed that the gain margin is equal to 7.7614 (17.8 dB) and the phase margin is equal to 67.8676. There is only one point at which one can obtain the phase margin of the system to be  $45^\circ$  and gain margin to be 3. This point is the intersection point of the stability boundary locus for  $A=3$  and the stability boundary locus for  $\phi = 45^\circ$ . This point corresponds to  $k_p = 0.0161$  and  $k_i = 21.1404$ . The step response of the system for different  $k_p$  and  $k_i$  values are indicated in Fig. 7.

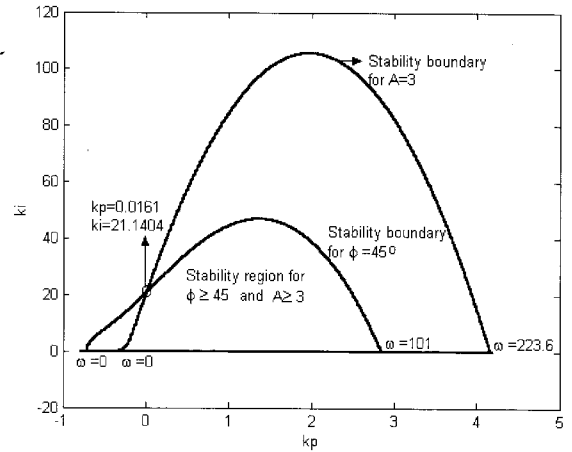


Fig. 6. Stability region for  $\phi \geq 45^\circ$  and  $A \geq 3$

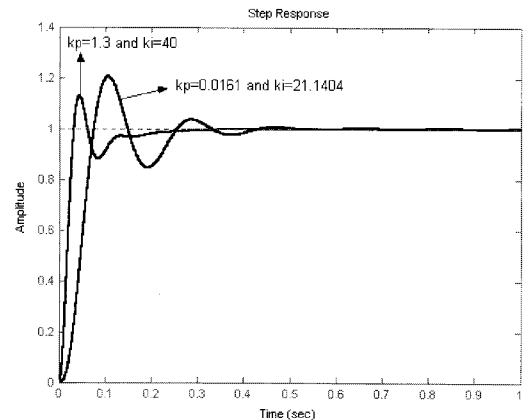


Fig. 7. Step response of the system for different  $k_p$  and  $k_i$  values in the stability region

### 4. Robustness Analysis

Parametric uncertainty in real systems is an unavoidable case and must be considered because nonlinear effects, environmental conditions, tolerance of the equipments, measurement faults etc. causes uncertainty. Thus, it is very important to take parametric uncertainty into consideration. It can be seen that the transfer function of the vehicle suspension system is a function of  $k_w, b, k_s, m_1$  and  $m_2$  [22]. All of these parameters can contain uncertainty. Consequently, taking uncertainties of the parameters of the transfer function of the vehicle suspension system into account provides more realistic design. Kharitonov theorem [20] is used for robust analysis of the system. In case of uncertainties, the proposed method can be applied to the control system as follows;

Consider a unity feedback system with a PI controller of Eq. (2) and an interval plant

$$G(s) = \frac{N(s)}{D(s)} = \frac{q_m s^m + q_{m-1} s^{m-1} + \dots + q_0}{p_n s^n + p_{n-1} s^{n-1} + \dots + p_0} \quad (28)$$

where  $q_i \in [\underline{q}_i, \overline{q}_i]$ ,  $i = 0, 1, \dots, m$  and  $p_i \in [\underline{p}_i, \overline{p}_i]$ ,  $j = 0, 1, \dots, n$ . Let the Kharitonov polynomials associated with  $N(s)$  and  $D(s)$  be respectively:

$$\begin{aligned} N_1(s) &= \underline{q}_0 + \underline{q}_1 s + \overline{q}_2 s^2 + \overline{q}_3 s^3 + \dots \\ N_2(s) &= \underline{q}_0 + \overline{q}_1 s + \overline{q}_2 s^2 + \underline{q}_3 s^3 + \dots \\ N_3(s) &= \overline{q}_0 + \underline{q}_1 s + \underline{q}_2 s^2 + \overline{q}_3 s^3 + \dots \\ N_4(s) &= \overline{q}_0 + \overline{q}_1 s + \underline{q}_2 s^2 + \underline{q}_3 s^3 + \dots \end{aligned} \quad (29)$$

And

$$\begin{aligned} D_1(s) &= \underline{p}_0 + \underline{p}_1 s + \overline{p}_2 s^2 + \overline{p}_3 s^3 + \dots \\ D_2(s) &= \underline{p}_0 + \overline{p}_1 s + \overline{p}_2 s^2 + \underline{p}_3 s^3 + \dots \\ D_3(s) &= \overline{p}_0 + \underline{p}_1 s + \underline{p}_2 s^2 + \overline{p}_3 s^3 + \dots \\ D_4(s) &= \overline{p}_0 + \overline{p}_1 s + \underline{p}_2 s^2 + \underline{p}_3 s^3 + \dots \end{aligned} \quad (30)$$

By taking all combinations of the  $N_i(s)$  and  $D_j(s)$  for  $i, j = 1, 2, 3, 4$ , the following sixteen Kharitonov plants family can be obtained

$$G_K(s) = G_{ij}(s) = \frac{N_i(s)}{D_j(s)} \quad (31)$$

where  $i, j = 1, 2, 3, 4$ . Define the set  $S(C(s)G(s))$  which contains all the values of the parameters of the controller  $C(s)$  which stabilize  $G(s)$ , then the set of all the stabilizing values of parameters of a PI controller which stabilize the interval plant of Eq. (28) can be written as

$$S(C(s)G(s)) = S(C(s)G_K(s)) = S(C(s)G_{11}(s)) \cap S(C(s)G_{12}(s)) \dots S(C(s)G_{44}(s)) \quad (32)$$

where  $G_K(s)$  represents the sixteen Kharitonov plant family which is given in Eq. (31) [21]. The transfer function of Eq. (18) can be written in the form of an interval plant as

$$G(s) = \frac{b_1 s + b_0}{a_4 s^4 + a_3 s^3 + a_2 s^2 + a_1 s + a_0} \quad (33)$$

where

$b_0 \in [18055555.56, 40625000]$ ,  $b_1 \in [1361111.11, 3062500]$ ,  $a_0 \in [18055555.56, 40625000]$ ,  $a_1 \in [1361111.11, 3062500]$ ,  $a_2 \in [47516.66, 71275]$ ,  $a_3 \in [441, 661.5]$  and  $a_4 = [1, 1]$ . Using the approach presented in Section 2, the stability regions of the 16 Kharitonov plants shown in Fig. 8 are obtained. From Fig. 8, it has been seen that the intersection of the stability regions that stabilize the uncertain vehicle suspension system is covered by the stability region of four Kharitonov plants, namely  $G_{33}(s)$ ,  $G_{23}(s)$ ,  $G_{43}(s)$  and  $G_{44}(s)$ . Thus, all the stabilizing values of  $k_p$  and  $k_i$  parameters can be computed from the intersection regions of the four Kharitonov plants that are shown in Fig. 9. The step responses of 16 Kharitonov plants for  $k_p = 3$  and  $k_i = 60$  obtained from Fig. 9 are shown in Fig. 10.

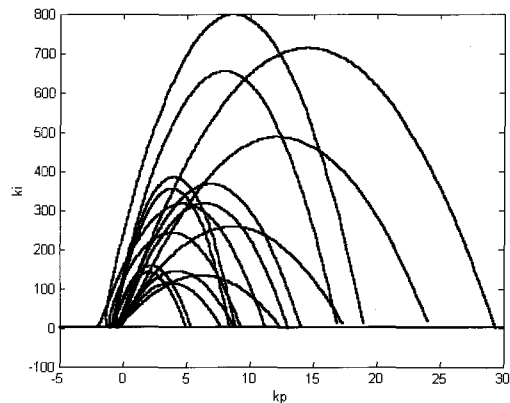


Fig. 8. Stability regions for sixteen Kharitonov plants

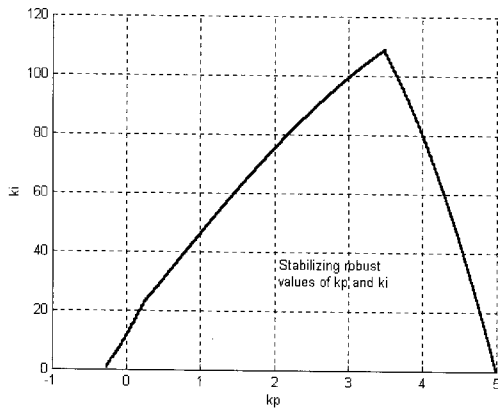


Fig. 9. All stabilizing robust  $k_p$  and  $k_i$  values

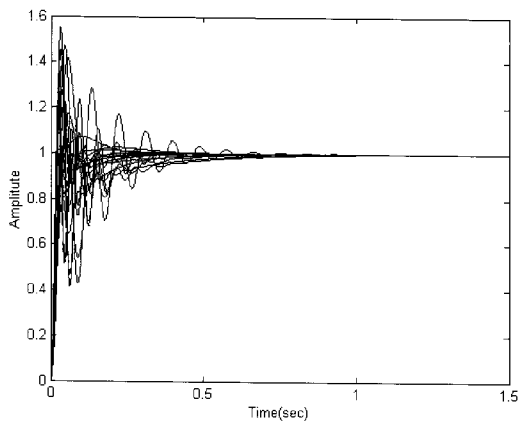


Fig. 10. Step responses of 16 Kharitonov plants for  $k_p = 3$  and  $k_i = 60$ .

### 5. Conclusions

In this paper, a PI controller design method for the vehicle suspension system has been presented. PI controller parameters that guarantee stability of the system are computed by using the stability boundary locus approach. Since the vehicle suspension system includes uncertainties, the stabilizing region of PI parameters for the control of the plant with uncertain parameters has been obtained. It has been revealed that the stability boundary locus method can effectively be used for design of the PI controller, which produces good results for the stability of suspension systems.

### References

[1] K. Matsumoto, K. Yamashita and M. Suzuki, "Robust  $H_\infty$  -output feedback control of decoupled automobile active suspension system", IEEE Trans.

on Automat. Contr., vol. 44, pp. 392-396, 1999.

[2] Elmadany, M., "Integral and state variable feedback controllers for improved performance in automotive vehicles", Comput Struct., vol. 42, no. 2, pp. 237-244, 1992.

[3] Isobe, T. and O. Watanabe, "New semi-active suspension controller design using quasi-linearization and frequency shaping", Control Eng. Pract., vol. 6, pp. 1183-1191, 1998.

[4] D'Amato, F.J. and D.E. Viassolo, "Fuzzy control for active suspension", Mechatronics, vol. 10, pp. 897-920, 2000.

[5] Kim H.J, H.S. Yaug and Y.P. Park, "Improving the vehicle performance with active suspension using road-sensing algorithm", Computers and Structure; vol. 80, pp. 1569-1577, 2002.

[6] Spentzas K. and A.K. Stratis "Design of a non-linear hybrid car suspension system using neural network", Mathematics and Computers in Simulation, vol. 60, pp. 369-378, 2002.

[7] Yao, G. Z., F. F. Yap, G. Chen, W. H. Li and S. H. Yeo, "MR damper and its application for semi-active control of vehicle suspension system", Mechatronics, vol. 12, pp. 963-973, 2002.

[8] Kuo Y. P. and T. H. S. Li, "GA-Based Fuzzy PI/PID Controller for Automotive Active Suspension System", IEEE Transactions on Industrial Electronics, vol. 46, pp. 1051-1056, December 1999.

[9] Onat C., İ. B. Küçükdemirel, Ş. Çetin and İ. Yüksek, "A comparison study of robust control strategies for automotive active suspension systems ( $H_\infty$ , LQR, Fuzzy Logic Control)", International Symposium on Innovations in Intelligent Systems and Applications, İstanbul-Turkey, pp. 291-294, 15-18 June 2005.

[10] Zhuang, M. and D. P. Atherton, "Automatic tuning of optimum PID controllers," IEE Proc. Part D, vol. 140, pp. 216-224, 1993.

[11] Astrom, K. J. and T. Hagglund, PID Controllers: Theory, Design, and Tuning. Instrument Society of America, 1995.

[12] Ho, M. T., A. Datta and S. P. Bhattacharyya, "A new approach to feedback stabilization," Proc. of the 35th CDC, pp. 4643-4648, 1996.

[13] Ho, M. T., A. Datta and S. P. Bhattacharyya, "A linear programming characterization of all stabilizing PID controllers," Proc. of Amer. Contr. Conf., 1997.

[14] Ho, M. T., A. Datta and S. P. Bhattacharyya, "Design of P, PI, and PID controllers for interval plants," Proc. of Amer. Contr. Conf., Philadelphia, June 1998.

[15] N. Tan, I. Kaya, C. Yeroglu and D. P. Atherton "Computation of stabilizing PI and PID controllers using the stability boundary locus", Energy Conversion and Management, vol. 47, pp. 3045-3058,

- 2006.
- [16] Söylemez, M. T., N. Munro and H. Baki, "Fast calculation of stabilizing PID controllers," *Automatica*, vol. 39, pp. 121-126, 2003.
- [17] Ackermann, J. and D. Kaesbauer, "Design of robust PID controllers," *European Control Conference*, pp. 522-527, 2001.
- [18] Shafiei, Z. and A. T. Shenton, "Frequency domain design of PID controllers for stable and unstable systems with time delay," *Automatica*, vol. 33, pp. 2223-2232, 1997.
- [19] Huang, Y. J. and Y. J. Wang, "Robust PID tuning strategy for uncertain plants based on the Kharitonov theorem," *ISA Transactions*, vol. 39, pp. 419-431, 2000.
- [20] Kharitonov, V. L., "Asymptotic stability of an equilibrium position of a family of systems of linear differential equations," *Differential Equations*, vol. 14, pp. 1483-1485, 1979.
- [21] Barmish, B. R., C. V. Holot, F. J. Kraus and R. Tempo, "Extreme points results for robust stabilization of interval plants with first order compensators," *IEEE Trans. on Automat. Contr.*, vol. 38, pp. 1734-1735, 1993.
- [22] Franklin, G.F., J.D. Powell and A. E. Naeni., "Feedback Control of Dynamic Systems", Prentice Hall, N.J., 2002.



#### **Celaleddin Yeroglu**

He received his B.S degree in Electrical and Electronic Engineering from Hacettepe University. He received his Ph.D degree in Computer Engineering from Trakya University. He worked for SISECAM, Trakya Automobile Glass Factory in Turkey as a Production Engineer for six years. His research interests are modeling and simulation of production systems, control engineering, and electrical discharge mechanisms.



#### **Nusret Tan**

He was born in Malatya, Turkey, in 1971. He received his B.Sc. degree in Electrical and Electronics Engineering from Hacettepe University, Ankara, Turkey, in 1994. He received his Ph.D. degree in Control Engineering from University of Sussex, Brighton, U.K., in 2000. He is currently working as an Associate Professor in the Department of Electrical and Electronics Engineering at Inonu University, Malatya, Turkey. His primary research interest lies in the area of systems and control.